



**HAL**  
open science

# VUV photopolymerization of ketene under interstellar conditions: from the dilute phase to the condensed phase

Mohamad Ibrahim, Jean-Claude Guillemin, Lahouari Krim

## ► To cite this version:

Mohamad Ibrahim, Jean-Claude Guillemin, Lahouari Krim. VUV photopolymerization of ketene under interstellar conditions: from the dilute phase to the condensed phase. *Monthly Notices of the Royal Astronomical Society*, 2022, 514 (3), pp.3754-3764. 10.1093/mnras/stac1452 . hal-03772620

**HAL Id: hal-03772620**

**<https://hal.science/hal-03772620>**

Submitted on 13 Mar 2023

**HAL** is a multi-disciplinary open access archive for the deposit and dissemination of scientific research documents, whether they are published or not. The documents may come from teaching and research institutions in France or abroad, or from public or private research centers.

L'archive ouverte pluridisciplinaire **HAL**, est destinée au dépôt et à la diffusion de documents scientifiques de niveau recherche, publiés ou non, émanant des établissements d'enseignement et de recherche français ou étrangers, des laboratoires publics ou privés.

VUV photo-polymerization of ketene under interstellar conditions: from the dilute phase to the condensed phase

Mohamad Ibrahim<sup>1</sup>, Jean-Claude Guillemin<sup>2</sup> and Lahouari Krim<sup>1\*</sup>

<sup>1</sup>*Sorbonne Université, CNRS, De la Molécule aux Nano-Objets: Réactivité, Interactions, Spectroscopies, MONARIS, 75005, Paris, France.*

<sup>2</sup>*Univ Rennes, Ecole Nationale Supérieure de Chimie de Rennes, CNRS, ISCR – UMR6226, F-35000 Rennes, France.*

\* *Corresponding author: Lahouari.krim@Sorbonne-universite.fr*

## Abstract

The photodecomposition of ketene under interstellar conditions and how the resulting photofragments may recombine in the 3-300 K temperature range could play an important role in investigations related to astrochemistry and astrobiology. Using a combination of bulk ice and rare-gas matrix isolation studies coupled to FTIR spectroscopy, the present work aims to understand the VUV photochemistry of CH<sub>2</sub>CO in solid phase to mimic the photochemistry of organic species trapped in the icy interstellar grains. We show that the photolysis of CH<sub>2</sub>CO depends strongly on the environments where it is trapped. The VUV photolysis of CH<sub>2</sub>CO/Ne in dilute phase leads to kinetically stable and instable species such as CO, C<sub>2</sub>H<sub>2</sub>, CH<sub>4</sub>, C<sub>2</sub>H<sub>4</sub>, C<sub>2</sub>H<sub>6</sub>, H<sub>2</sub>CO, CH<sub>3</sub>CHO, HCCO, C<sub>2</sub>O, C<sub>3</sub>O and C<sub>4</sub>O. However, the same experiment carried out in condensed phase shows that the photolysis of CH<sub>2</sub>CO ice produces mainly an organic residue which is directly observed at 10 K and remains stable in solid phase at 300 K. The IR spectroscopy analysis suggests that the resulting organic residue could be a polyketone formed at 10 K through the VUV photo-polymerization of ketene.

**Keywords:** astrochemistry, molecular processes, methods: laboratory: molecular, techniques: spectroscopic, ISM: molecules

## 1. Introduction

The probe of the interstellar medium (ISM) components and processes that occur in it, yield to different molecular species, and more specifically, organic molecules in general and prebiotic species in particular. All these chemical species can be present either in the gas phase and in the solid phase (locked in the icy mantles on dust grains). More than a few molecules have been detected in the ISM and circumstellar shells including molecules from 2 atoms to 13 atoms and more than 70 species containing six or more atoms of C, H, O, or N (Herbst & van Dishoeck 2009) are called complex organic molecules (COM). Among these simple or complex organic species, ketene ( $\text{CH}_2\text{CO}$ ), a molecule of astrophysical and astrobiology interests, and detected in different regions of the Universe, has been a subject of several experimental (Chen et al 1988, Chen & Moore 1990, Chen & Moore 1990, Kim et al 1991, Lovejoy et al 1992, Liu et al. 1992, Moreno et al. 1994, Kim et al. 1995, Morgan et al. 1996, Castillejo et al 1998, Glass et al. 2000, Feltham et al. 2003, Liu et al. 2005, Fockenberg 2005) and theoretical (Yamabe et al. 1978, Allen & Schaefer (1986; 1988), Klippenstein & Marcus 1989, Yu & Klippenstein 1991, Klippenstein et al. 1996, Cui & Morokuma 1997, Yarkony 1999, Forsythe et al. 2001, Kaledin et al 2001, Cole & Balint-Kurti 2003, Liu et al 2006, Ogihara et al. 2011, Ogihara et al. 2011, Xiao et al. 2013) investigations. From an astronomical point of view, ketene has been first observed in the direction of the star formation region SgrB2 with abundance of  $1.7 \times 10^{-10}$  molecules  $\text{cm}^{-2}$  (Turner et al. 1977). Afterwards, Johansson et al. (1984) have reported its detection in Orion KL molecular clouds, while Matthews & Sears (1986) have shown that  $\text{CH}_2\text{CO}$  may be present in both Sgr B2 and TMC-1. A few years later, Irvine et al. (1989) and Ohishi et al. (1991) have confirmed the presence of this molecule in TMC-1 with an abundance of  $10^{-9}$  molecules  $\text{cm}^{-2}$ . Later, several observations have concluded that ketene was present in several clouds including translucent clouds CB 17, CB 24, and CB 228 (Turner et al. 1999), extragalactic sources (Muller et al. 2011) and prestellar cores (Bacmann et al. 2012). Associated to these astronomical observations, different laboratory studies have been carried out to characterize the formation and reactivity of  $\text{CH}_2\text{CO}$  under ISM conditions. Hudson & Loeffler (2013) investigated through energetic mechanisms the formation of  $\text{CH}_2\text{CO}$  at 10 K in interstellar ice analogs containing  $\text{C}_2\text{H}_2$ ,  $\text{O}_2$ ,  $\text{CH}_4$ ,  $\text{H}_2\text{O}$  and  $\text{CO}_2$ , using proton irradiation (0.8 MeV) and  $\text{Ly}\alpha$  photolysis. By means of two complementary detection techniques, in situ FTIR spectroscopy and single photoionization TPD ReTOF mass

spectrometry, ketene has mostly been identified in CH<sub>4</sub>-CO ices upon its exposure to energetic electrons at 5.5 K (Maity et al 2014). Further, Abplanalp and Kaiser (2019) have investigated the ketene formation in ice mixtures containing carbon monoxide and ethane, ethylene or acetylene exposed to ionizing radiations. Similarly, Turner et al. (2020) have reported an experimental and theoretical investigation into the formation of ketene and ethynol in CO-H<sub>2</sub>O interstellar ice analogs irradiated with 5 keV electrons. Chuang et al. (2021) identified organic molecules of the form of C<sub>2</sub>H<sub>n</sub>O such as ketene by performing 200 keV H<sup>+</sup> radiolysis chemistry on C<sub>2</sub>H<sub>2</sub>:H<sub>2</sub>O ice mixtures. Additionally, several matrix isolation studies have been carried out to investigate the formation of ketene using different chemical precursors and energetic sources. In this context, Haller&Pimentel (1962) investigated the photolysis of N<sub>2</sub>O-C<sub>2</sub>H<sub>2</sub>/Ar at 1470 Å while Hawkins & Andrews (1983) that of O<sub>3</sub>-C<sub>2</sub>H<sub>4</sub>/Ar at 2200 Å. More recently, the formation of ketene isolated in solid noble-gas or molecular matrices have been reported through the UV photolysis at 20 K of C<sub>2</sub>H<sub>4</sub>O/Ar and C<sub>2</sub>H<sub>4</sub>O/N<sub>2</sub> (Shriver et al 2004). Zsimev et al. (2020) reported the CH<sub>2</sub>CO formation through the X-ray irradiation at 5 K of C<sub>2</sub>H<sub>2</sub>-H<sub>2</sub>O trapped in various solids (Ar, Kr, Xe). In addition to these mechanisms involving energetic sources, Chuang et al. (2020) have shown that non-energetic processing of C<sub>2</sub>H<sub>2</sub> ice interacting with H-atoms and OH-radicals provide other formation routes to ketene. In the same way, Fedoseev et al. (2021) have reported that CH<sub>2</sub>CO may also be formed through a co-deposition at 10 K of CO, H<sub>2</sub>O, C- and H- atoms. Besides to its formation, many investigations have been devoted to CH<sub>2</sub>CO dissociation. Yamabe & Morokuma (1978) carried out *ab initio* calculations for the photodissociation of ketene which leads to CH<sub>2</sub> and CO as main photoproducts. Later, Allen & Shaeffer (1986) have performed theoretical investigations for the geometry and vibrational frequencies of three state of ketene and two transition states for dissociation. Then, an *ab initio* potential energy surface has been developed by Yu & Klippenstein (1991) to explore the energetics for the dissociation of CH<sub>2</sub>CO into CH<sub>2</sub> and CO fragments. In this paper, we present a combination of bulk ice and neon matrix isolation studies to examine the photochemistry of CH<sub>2</sub>CO from the dilute to the condensed phase.

## 2. Experimental section

The experimental setup used in the present study has been described in previous articles (Jonusas&Krim, 2017), thus only features are mentioned hereafter. The experiments are performed under ultra high vacuum at  $10^{-10}$  mbar. Samples are condensed onto a cryogenic metal mirror maintained at low temperature. This temperature is kept stable using a pulsed tube closed-cycle cryogenerator (Sumitomo cryogenics F-70) and programmable temperature controller (Lakeshore 336). Our samples are characterized spectrally by recording infrared spectra in the transmission-reflection mode between 5000 and 500  $\text{cm}^{-1}$ , with a resolution of 0.5  $\text{cm}^{-1}$ , using a Bruker 120 FTIR spectrometer. Ketene is prepared by thermolysis of acetic anhydride at 900°C under 0.1 mbar and selective trapping of the formed acetic acid in a trap cooled to -60°C. The gaseous flow containing pure ketene is then condensed in a second trap immersed in a liquid nitrogen bath. Ketene is stored under vacuum in a reservoir at -196°C in liquid nitrogen. A temperature of -110°C is needed to evaporate and introduce  $\text{CH}_2\text{CO}$  into the injection ramp. Such a temperature is reached and maintained by adding liquid nitrogen in an ethanol bath. Afterwards, the frozen ketene is partially evaporated into the injection ramp by monitoring and stabilizing the bath temperature at -110°C. Pressures in the injection ramp are measured with a digital Pirani gauge, while the fractions of ketene gas injected into the experimental chamber are controlled using a leak valve. The solid samples are then irradiated at low temperature during 30 min using a vacuum ultra-violet (VUV) light source (Hamamatsu L10706 UV, 25% at 121 nm ~ 10.1 eV and 75% at 160 nm ~ 7.7 eV) with a total flux of  $10^{15}$  photons  $\text{cm}^{-2}\text{s}^{-1}$ . The photolysis of the  $\text{CH}_2\text{CO}$  has been carried out using two different experimental methods:

*Photolysis of ketene in dilute phase:* The first experiment consists on isolating ketene in a neon matrix. The sample is prepared by co-condensing  $\text{CH}_2\text{CO}/\text{Ne} = 1/100$  mixtures onto a substrate at 3K. Then the irradiated matrix is heated progressively from 3 to 20 K and cooled down to 10 K to remove the neon atoms and recover an irradiated  $\text{CH}_2\text{CO}$  ice which can be compared to  $\text{CH}_2\text{CO}$  ice irradiated at 10 K performed with the second experimental method.

*Photolysis of ketene in the condensed phase:* This second experiment consists on the formation of a ketene ice analog using  $\text{CH}_2\text{CO}$  taken from the gas phase and condensed directly on substrate maintained at 10 K. The resulting ice is characterized before and after irradiation.

For both experimental methods, the irradiated  $\text{CH}_2\text{CO}$  ice is then heated progressively from 10 to 300 K to investigate the thermally induced reactions.

### 3. Results

**a) Photolysis of ketene in diluted phase:** For a given chemical reaction, neon matrix isolation allows a clear characterization of the reactants, reaction intermediates and products, showing separate and resolved IR signatures for each trapped species, which signatures are easily identifiable as they are close to those measured in the gas phase. Figure 1a shows the IR spectrum of  $\text{CH}_2\text{CO}$  isolated in neon matrix at 3 K before irradiation. The assignments of the main vibrational modes of  $\text{CH}_2\text{CO}$  are reported in table 1 and compared to previous experimental and theoretical studies.

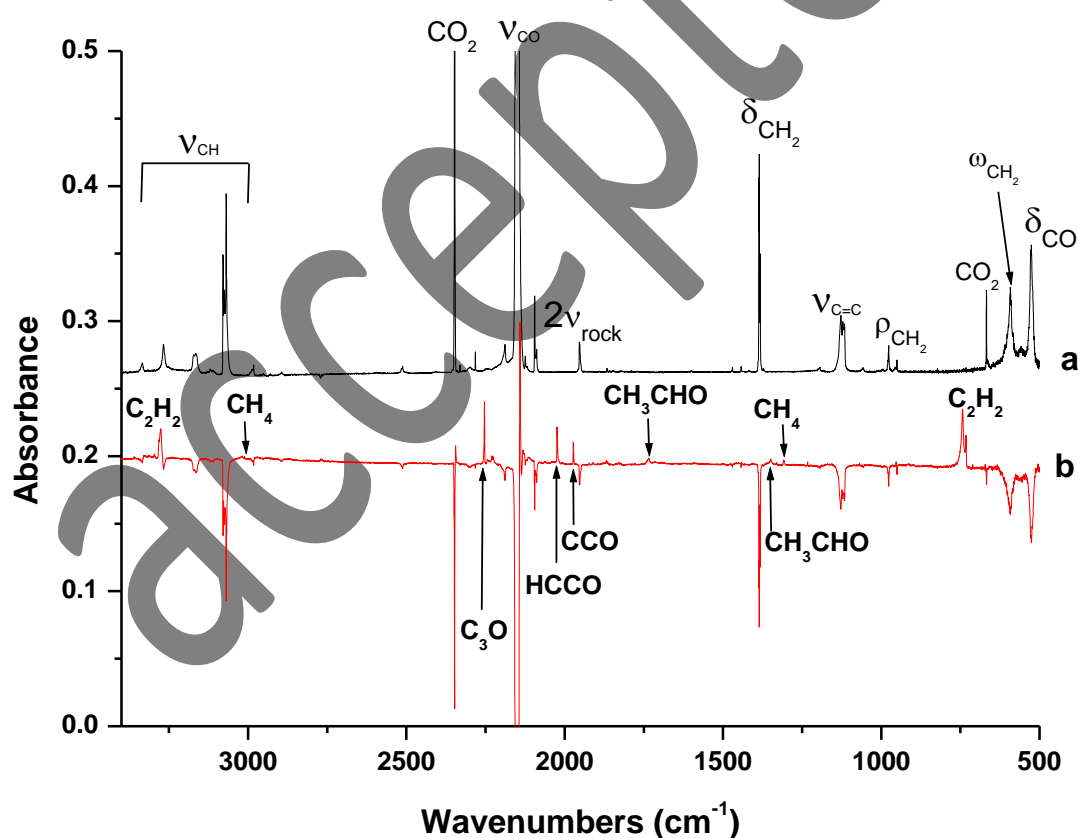


Figure 1: a) IR spectrum of  $\text{CH}_2\text{CO}$  isolated in neon matrix at 3 K before irradiation. b) IR difference spectrum after and before photolysis.

Table 1. Infrared absorption bands with assignments of CH<sub>2</sub>CO in matrix isolation Ne and Ar.

CH <sub>2</sub> CO in Ne	CH <sub>2</sub> CO in Ar <sup>a,b,c</sup>	CH <sub>2</sub> CO Theo <sup>c</sup>	Vibrational modes
3164.1	3155	3297	C-H str
3069.2	3062	3192	C-H str
2152.2	2142	2181	C=O str
2088.6	2085		<sup>13</sup> C=O str
1953.5	1947		Overtone(CH <sub>2</sub> rock)
1382.7	1381	1411	H-C-H bend
1116	1115	1148.4	C=C str
976.4	974	989.6	CH <sub>2</sub> rock
592.3	587.5	587.6	CH <sub>2</sub> wag
526		506.8	C=C=O bend
		434.5	C=C=O bend

a-Moore&Pimentel 1963

b-Hawkins&andrews 1983

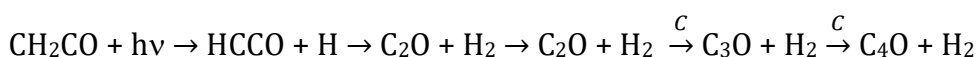
c-Turner et al. 2020

CH<sub>2</sub>CO trapped in neon matrix is characterised by four spectral regions located at 3400-3000 cm<sup>-1</sup>, 2200-2000 cm<sup>-1</sup>, 1500-900 cm<sup>-1</sup> and 700-500 cm<sup>-1</sup>. The most intense IR signal is positioned at 2152.2 cm<sup>-1</sup> and assigned to CO stretching mode. Figure 1b shows the IR difference spectrum after and before photolysis. The negative peaks in the spectrum indicate that almost 75 % of ketene is consumed to form several photoproducts with positive IR signatures which may be assigned based on the previous matrix isolation and gas phase studies. Among the photoproducts detected, we are able to observe highly-reactive species such as radicals and reaction intermediates which are stabilized in the neon matrix. Table 2 summarizes most of the IR signals observed and their assignments based on the literature data. Starting from the most intense IR signals detected after photolysis, we distinguish two absorption bands around 730 and 3280 cm<sup>-1</sup> which may be associated to C<sub>2</sub>H<sub>2</sub> formation. Wu et al. (2010) investigated the neon matrix isolation of C<sub>2</sub>H<sub>2</sub> which shows four intense IR lines, located at 731.8, 1329.9, 3283.6 and 3296.8 cm<sup>-1</sup> and corresponding to vibrational modes  $\nu_5$ ,  $\nu_4+\nu_5$ ,  $\nu_3$ , and  $\nu_2+\nu_4+\nu_5$ , respectively. They also detected two IR peaks at 745.0 and 3269.7 cm<sup>-1</sup>, characteristic of C<sub>2</sub>H<sub>2</sub> dimer. Under our experimental conditions the absorption band detected after photolysis

around  $730\text{ cm}^{-1}$  is actually compound of one sharp line and one broad band at  $732.2$  and  $743.6\text{ cm}^{-1}$ , respectively, showing that the irradiation of ketene is a source of  $\text{C}_2\text{H}_2$  monomer and also of  $\text{C}_2\text{H}_2$  aggregate. Similarly, the IR signal around  $3280\text{ cm}^{-1}$  confirms such a hypothesis, where three IR lines are observed at  $3275.9$ ,  $3281.6$ ,  $3296.7\text{ cm}^{-1}$  and may be assigned to  $\text{C}_2\text{H}_2$  monomer trapped in neon matrix, and one peak at  $3268.1\text{ cm}^{-1}$  which may be due to  $\text{C}_2\text{H}_2$  dimer. All the IR lines of  $\text{C}_2\text{H}_2$  we observe are in good agreements with the results reported by Wu et al (2010). Additionally, the combination band  $\nu_4+\nu_5$  measured by Wu et al (2010) at  $1329.9\text{ cm}^{-1}$  is also detected under our experimental conditions at  $1330.0\text{ cm}^{-1}$ . Furthermore, by coupling IR-spectra of acetylene isolated in argon matrix and quantum chemical calculations, Golovkin et al. (2013) reported that molecular complexes such as  $(\text{C}_2\text{H}_2)_2$ ,  $(\text{C}_2\text{H}_2)_3$  and  $(\text{C}_2\text{H}_2)_4$  may form at low temperature and can be identified through characteristic IR signatures in the  $3200\text{-}3300\text{ cm}^{-1}$  and  $760\text{-}620\text{ cm}^{-1}$  spectral regions. They showed that the absorption band of  $\text{C}_2\text{H}_2$  monomer is observed at  $736.5\text{ cm}^{-1}$  and those of acetylene aggregates are blue or red shifted. They observed the acetylene dimer at  $745.0$  and  $750.5\text{ cm}^{-1}$ , the trimer at  $756.8$  and  $759\text{ cm}^{-1}$  while the bands due to the tetramer overlapping with those of condensed acetylene, at  $762.4$ ,  $764.8$  and  $770.4\text{ cm}^{-1}$ . Similarly, in the C-H stretching region, Golovkin et al. showed that the IR signal due  $\text{C}_2\text{H}_2$ , is located at  $3287.9\text{ cm}^{-1}$ , while the absorption bands of  $(\text{C}_2\text{H}_2)_2$  are observed at  $3284.3$  and  $3268.7$  and those of  $(\text{C}_2\text{H}_2)_3$  at  $3265.3$  and  $3262.6\text{ cm}^{-1}$ . One wide band at  $3255\text{ cm}^{-1}$  has been assigned to  $(\text{C}_2\text{H}_2)_4$ . From this study we notice that the spectral shifts of the absorption bands of acetylene are mainly due to the formation of  $(\text{C}_2\text{H}_2)_2$ ,  $(\text{C}_2\text{H}_2)_3$  and  $(\text{C}_2\text{H}_2)_4$ . In the same context, by investigating the ion irradiation of acetylene ice, Pereira et al. (2020) also showed that absorption bands of  $\text{C}_2\text{H}_2$  exhibit spectral shifts and shape changing depending on the thickness of the sample and the ion beam fluences, which are probably due to formation of aggregates of acetylene. This illustrates that under our experimental conditions, the main reaction product formed during the photolysis of  $\text{CH}_2\text{CO}$  diluted in neon matrix is  $\text{C}_2\text{H}_2$  which may be present as monomeric or aggregated species.

Three other intense IR lines located in the CO stretching region of  $\text{CH}_2\text{CO}$  are observed at  $2253.5$ ,  $2024.4$  and  $1972.9\text{ cm}^{-1}$  and assigned to  $\text{C}_3\text{O}$ ,  $\text{HCCO}$  and  $\text{C}_2\text{O}$  radicals, respectively. This indicates that the photolysis of ketene in diluted phase leads, in addition to  $\text{C}_2\text{H}_2$ , to a dehydrogenation process. Zasimov et al. (2022) investigated the

radiation induced transformation of acetaldehyde trapped in neon matrix. They showed that the UV radiation of CH<sub>3</sub>CHO leads to CH<sub>2</sub>CHOH, CH<sub>3</sub>O, CH<sub>3</sub>, CH<sub>2</sub>CO, HCCO and C<sub>2</sub>O trapped in neon matrix and characterised by the main IR lines at 1077.7, 1884.3, 607.6, 2151.3, 2024.4 and 1972.9 cm<sup>-1</sup>, respectively. However, we did not detect a signal at 1077.7 cm<sup>-1</sup> to support the formation of vinyl alcohol (CH<sub>2</sub>CHOH) isolated in neon matrix. We show, under our experimental conditions, that the photolysis of ketene leads to species absorbing at 2024.4 and 1972.9 cm<sup>-1</sup> and they may be assigned to HCCO and C<sub>2</sub>O radicals, respectively. In addition to the signal at 1972.9 cm<sup>-1</sup> due to ν<sub>1</sub> vibrational mode of C<sub>2</sub>O, another weak signal is detected at 1069.0 cm<sup>-1</sup> and could be tentatively assigned to ν<sub>3</sub> mode of C<sub>2</sub>O radical. Investigations on rotationally resolved infrared spectrum between 1030 and 1105 cm<sup>-1</sup> (Abusara et al. 2004) reported the spectral position of the ν<sub>3</sub> mode of C<sub>2</sub>O in the <sup>1</sup>Δ state at 1082 cm<sup>-1</sup>. Moreover, the intense signal at 2253.5 cm<sup>-1</sup> could be due to C<sub>3</sub>O which may result from secondary reactions such as C<sub>2</sub>O + C. Another IR line with relative low intensity is detected at 1909.1 cm<sup>-1</sup> and could also be assigned to C<sub>3</sub>O. Such assignments are confirmed by previous studies carried out by Botschwina & Reisenauer (1991) and Rouillé et al. (2020). In fact, Botschwina & Reisenauer (1991) investigated the argon matrix isolation of C<sub>3</sub>O which is characterized by two IR signals: an intense line at 2243.0 cm<sup>-1</sup> and another medium line located at 1907 cm<sup>-1</sup>. The detection of such a species would suggest the presence of carbon atoms in the irradiated sample. Moreover, another species similar to C<sub>3</sub>O is also detected under our experimental conditions but with less intense lines at 2224.7 and 1922.1 cm<sup>-1</sup>. Such a species is C<sub>4</sub>O which has been already investigated by Maier et al. (1988) through an argon matrix isolation study. They reported that C<sub>4</sub>O has two characteristic IR signals at 2221.7 and 1922.7 cm<sup>-1</sup> which are close to the IR lines we measure during the photolysis of CH<sub>2</sub>CO trapped in neon matrix. Similarly to C<sub>3</sub>O formation, C<sub>4</sub>O could result from interactions between carbon atoms and C<sub>2</sub>O:



As shown in figure 1b, and in figure 2 which is a zoom of the IR difference spectrum after and before photolysis at 3K, two weak absorption bands are observed at 1348.8 and 1738.2 cm<sup>-1</sup> and assigned to CH<sub>3</sub>CHO. Another weak IR signal is detected at 3020.5 cm<sup>-1</sup> and assigned to CH<sub>3</sub>CHO. These assignments are based on Zasimov et al. (2022) investigations for the photolysis of CH<sub>3</sub>CHO isolated in neon matrix. This shows that in

addition to a dehydrogenation process of CH<sub>2</sub>CO to form HCCO and CCO during the photolysis, the dissociated H atoms interact with ketene to form acetaldehyde through a successive hydrogenation process:



In fact, as mentioned above, Zasimov et al. (2022) showed that acetaldehyde trapped in neon can be characterized by three IR lines at 3022.8, 1738.1 and 1349.0 cm<sup>-1</sup> and its photodecomposition leads to CH<sub>3</sub>O characterized through an absorption peak at 1884.3 cm<sup>-1</sup>. Under our experimental conditions, in addition to CH<sub>3</sub>CHO detection, we have also observed a weak IR signal at 1880.4 cm<sup>-1</sup> which could be tentatively assigned to CH<sub>3</sub>O radical.

A few absorption bands with relative less intensity are observed at 1308.1, 3011.5 cm<sup>-1</sup> and at 1500.0, 1740.0 cm<sup>-1</sup> and which may correspond to CH<sub>4</sub> and H<sub>2</sub>CO, respectively. The formation of CH<sub>4</sub> and H<sub>2</sub>CO indicates that in addition to the simultaneous dehydrogenation and hydrogenation of ketene to form HCCO and C<sub>2</sub>O radicals and CH<sub>3</sub>CHO, respectively, another dissociative pathway transforms CH<sub>2</sub>CO into CH<sub>2</sub> + CO which reacting with H atoms would lead to CH<sub>4</sub> and H<sub>2</sub>CO, respectively. The hydrogenation of the resulting CO leads obviously to H<sub>2</sub>CO which is characterized by two IR lines observed in figure 2 at 1500.0, 1740.0 cm<sup>-1</sup>. However, we also observe a signal at 1866.1 cm<sup>-1</sup> which can be assigned to HCO trapped in neon matrix. In our previous study (Pirim & Krim 2011) for the CO + H reaction isolated in neon matrix, we detected HCO and H<sub>2</sub>CO at 1864.8 and 1740.5 cm<sup>-1</sup>, respectively.

Two radical species have not been observed because their IR signals overlap with the absorption bands of ketene. The region around 607 cm<sup>-1</sup> which is characteristic of CH<sub>3</sub> radical (Zasimov et al. 2022) and those around 963 and 3190 cm<sup>-1</sup> where CH<sub>2</sub> IR signal would be detected (Petek et al. 1989; Marshall & McKellar 1986). However, this does not exclude the formation of such radicals under our experimental conditions, since CH<sub>2</sub> and CH<sub>3</sub> are reaction intermediates of CH<sub>4</sub> for the reactions CH<sub>3</sub> + H and CH<sub>2</sub> + 2H. On the other side, we have detected the CH radical at 2733.3 cm<sup>-1</sup> which is in good agreement with Wu et al. (2009) who reported the vibration of CH in neon matrix at 2732.9 cm<sup>-1</sup>.

Table 2. Vibrational assignments of the main photoproducts resulting from the VUV photolysis ketene isolated in Ne matrix.

Bands detected $\text{cm}^{-1}$	Assignments	Ref
732.2/743.6	$\text{C}_2\text{H}_2$	Lin et al 2014 and Wu et al 2010
1308.1	$\text{CH}_4$	Wu et al. 2009
1348.8	$\text{CH}_3\text{CHO}$	Zasimov et al. 2022
1500,0	$\text{H}_2\text{CO}$	Khoshkhoo et al. 1973
1740,0	$\text{H}_2\text{CO}$	Pirim et al. 2011
1738.2	$\text{CH}_3\text{CHO}$	Zasimov et al. 2022
1866.1	$\text{HCO}$	Pirim et al. 2011
1880.4	$\text{CH}_3\text{CO}$	Zasimov et al. 2022
1909.1	$\text{C}_3\text{O}$	Botschwina&Reisenauer 1991
1922.1	$\text{C}_4\text{O}$	Maier et al. 1988
1972.9	$\text{CCO}$	Zasimov et al. 2022
2024.4	$\text{HCCO}$	Zasimov et al. 2022
2226.6	$\text{C}_4\text{O}$	Maier et al. 1988
2253.5	$\text{C}_3\text{O}$	Rouillé et al 2020
2733.3	$\text{CH}$	Wu et al. 2009
3011.5	$\text{CH}_4$	Wu et al. 2009
3020.5	$\text{CH}_3\text{CHO}$	Zasimov et al. 2022
3268.1/3275.9/3281.6/3296.7	$\text{C}_2\text{H}_2$	Lin et al. 2014 and Wu et al 2010

Finally two weak IR lines located at 1828.9 and 1823.2  $\text{cm}^{-1}$  in figure 2 are tentatively assigned to cyclopropanone  $\text{C}_3\text{H}_4\text{O}$ . Singmaster & Pimentel (1989) showed that cyclopropanone trapped in argon matrix absorbs at 1823.4 and 1815.1  $\text{cm}^{-1}$  while ab initio calculations carried out by Savchenkova et al. (2019) demonstrated that  $\text{CH}_2$ , which may derive from the photodissociation of ketene would interact with  $\text{CH}_2\text{CO}$  to form cyclopropanone  $\text{CH}_2 + \text{CH}_2\text{CO} \rightarrow \text{C}_3\text{H}_4\text{O}$ . Table 2 gathers the main photoproducts resulting from the VUV photolysis of ketene isolated in Ne matrix.

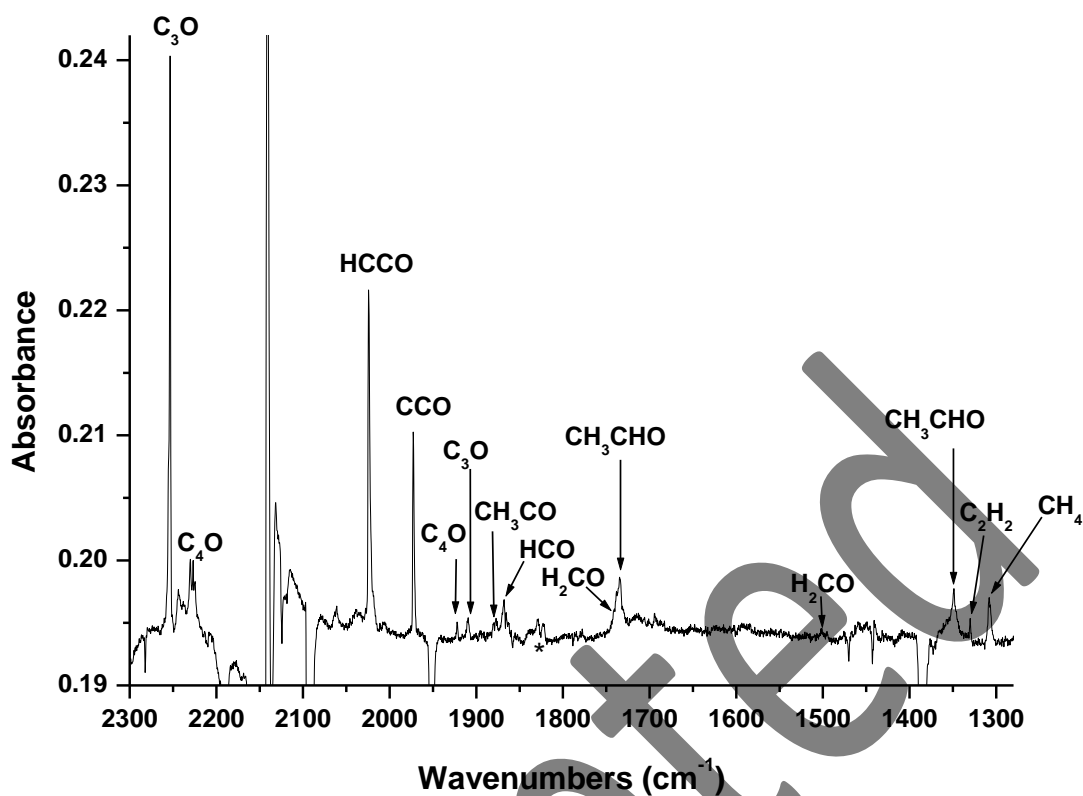


Figure 2: zoom of the IR difference spectrum after and before photolysis at 3K. \* The two peaks at 1828.9 and 1823.2  $\text{cm}^{-1}$  are tentatively assigned to cyclopropanone (see the text).

The heating of  $\text{CH}_2\text{CO}/\text{Ne}$  irradiated sample to higher temperature (20 K) enables to evaporate neon atoms and to retrieve an interstellar ice analog where all the reaction products are trapped in ketene ice. After the total sublimation of neon atoms at 20 K, the sample is cooled down to 10 K (figure 3b) and compared to a pure  $\text{CH}_2\text{CO}$  ice formed at 10 K (figure 3a).

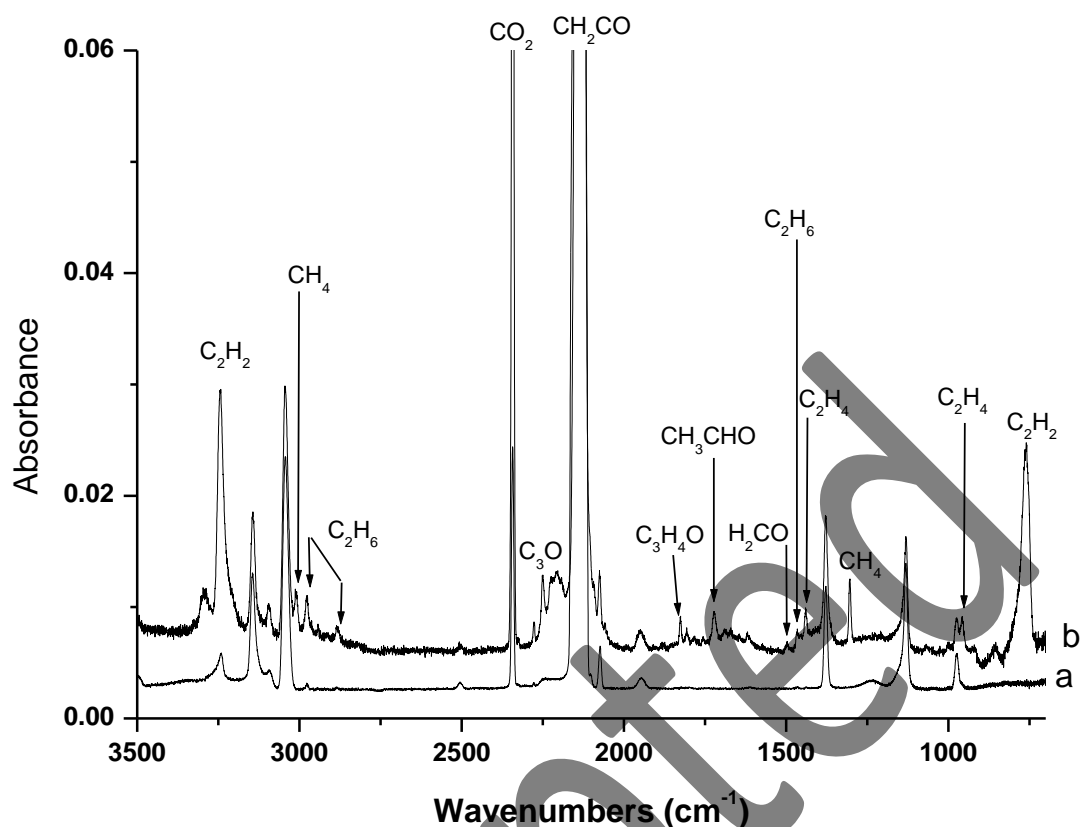


Figure 3: a) CH<sub>2</sub>CO ice formed at 10 K. b) IR spectrum recorded at 10 K after photolysis of CH<sub>2</sub>CO isolated in neon matrix at 3 K followed by a total sublimation of neon atoms at 20 K, then a cooling down to 10 K.

We notice that at 20 K the neon matrix disappears completely, the IR signals due to radical species such as HCCO and C<sub>2</sub>O are vanished while those due to stable molecules such as CH<sub>2</sub>CO, C<sub>2</sub>H<sub>2</sub> and CH<sub>3</sub>CHO are slightly shifted and become wider, indicating an evolution from a diluted to condensed phase. In fact, the two bands at 2024.4 and 1972.9 cm<sup>-1</sup> attributed HCCO and C<sub>2</sub>O radicals disappear during the heating (figure 3b), while that at 2253.4 cm<sup>-1</sup> and assigned to C<sub>3</sub>O is considerably reduced. All the common signals appearing in both spectra of figures 3a and 3b are due to CH<sub>2</sub>CO ice. The bands corresponding to C<sub>2</sub>H<sub>2</sub> becomes broadband and shift to 760 and 3244 cm<sup>-1</sup> (Chuang et al 2020). The band at 1308.1 cm<sup>-1</sup> corresponding to CH<sub>4</sub> shift to 1304 cm<sup>-1</sup>, and that assigned to CH<sub>3</sub>CHO at 1738.2 cm<sup>-1</sup> shifts to 1721 cm<sup>-1</sup> (Hudson & Ferrante 2020).

The comparison of the IR spectrum of the irradiated CH<sub>2</sub>CO/Ne sample after the evaporation of neon atoms with that of a pure CH<sub>2</sub>CO ice formed at 10 K would allow to distinguish all the IR signals of CH<sub>2</sub>CO ice from those of the final photoproducts remained trapped in CH<sub>2</sub>CO ice. Figure 3 shows such a comparison where at 10 K we are able to distinguish the signals due to CH<sub>4</sub> (3012 and 1304 cm<sup>-1</sup>), to H<sub>2</sub>CO (1500 cm<sup>-1</sup>) and to CH<sub>3</sub>CHO (1721 cm<sup>-1</sup>). However, the most intense IR signals of the photoproducts are still due to C<sub>2</sub>H<sub>2</sub> observed at 3244 and 760 cm<sup>-1</sup>. Other non-oxygenated species such as C<sub>2</sub>H<sub>4</sub> and C<sub>2</sub>H<sub>6</sub> are easily identifiable in figure 3b and are probably formed during the heating of the irradiated sample. The two IR lines located at 1828.9 and 1823.2 cm<sup>-1</sup> and assigned to C<sub>3</sub>H<sub>4</sub>O, a reaction product from CH<sub>2</sub> + CH<sub>2</sub>CO, are shifted to 1825 cm<sup>-1</sup>.

As a first conclusion the photolysis of ketene in diluted phase in neon matrix at 3 K leads mainly to radical species such as HCCO, CCO, C<sub>3</sub>O, C<sub>4</sub>O, HCO and CH<sub>3</sub>CO and to stable molecules, namely, H<sub>2</sub>CO, CH<sub>3</sub>CHO, CH<sub>4</sub>, C<sub>2</sub>H<sub>2</sub>, C<sub>3</sub>H<sub>4</sub>O and certainly CO which absorbs at 2140 cm<sup>-1</sup>, the same spectral region as CH<sub>2</sub>CO. After the total sublimation of neon atoms at 20 K and the cooling down of sample at 10 K to recover the photoproducts trapped in CH<sub>2</sub>CO ice, most of the radical species disappear while H<sub>2</sub>CO, CH<sub>3</sub>CHO, CH<sub>4</sub>, C<sub>2</sub>H<sub>2</sub> and C<sub>3</sub>H<sub>4</sub>O remain in the ice with other non-oxygenated species such as C<sub>2</sub>H<sub>6</sub> and C<sub>2</sub>H<sub>4</sub> which may form during the sublimation of neon atoms.

**b) Photolysis of ketene in condensed phase:** A ketene ice is formed at 10 K, then the solid sample is characterized before (figure 4a) and after irradiation (figure 4b). Table 3 sums the main vibrational modes of ketene ice. Table 3 gathers the main absorption bands of CH<sub>2</sub>CO ice and their assignments based on the neon matrix isolation study exposed above.

Table 3. Infrared absorption bands of CH<sub>2</sub>CO ice at 10 K.

Frequency	Vibrational modes
3143.3	C-H str
3042.2	C-H str
2115.6	C=O str
2072.4	<sup>13</sup> C=O str
1376.9	H-C-H bend
1131.0	C=C str
974.8	CH <sub>2</sub> rock
600.3	CH <sub>2</sub> wag
519.0	C=C=O bend

The IR spectrum of figure 4b shows the IR signatures related to CH<sub>2</sub>CO and all the photoproducts formed under our experimental conditions. As for the photolysis in neon matrix, the irradiation of ketene ice during 30 min indicates that almost 75 % of CH<sub>2</sub>CO is consumed to form several photoproducts. Although we are able to quantify the decrease of the IR intensities of ketene absorption bands by comparing the spectra of figures 4a and 4b, we cannot easily list all the photoproducts formed during the photolysis in the condensed phase. The comparison between figures 4a and 4b allows only to distinguish the IR lines of the reactant from those of the products without bringing information about their nature. We notice that the IR signals of the resulting photoproducts are completely different from those obtained in the first experiment. Most of the absorption bands of the photoproducts are broad and located in 2000-700 cm<sup>-1</sup> spectral region with a noteworthy absence of signals at 3244 and 760 cm<sup>-1</sup> due to C<sub>2</sub>H<sub>2</sub> trapped in ketene ice.

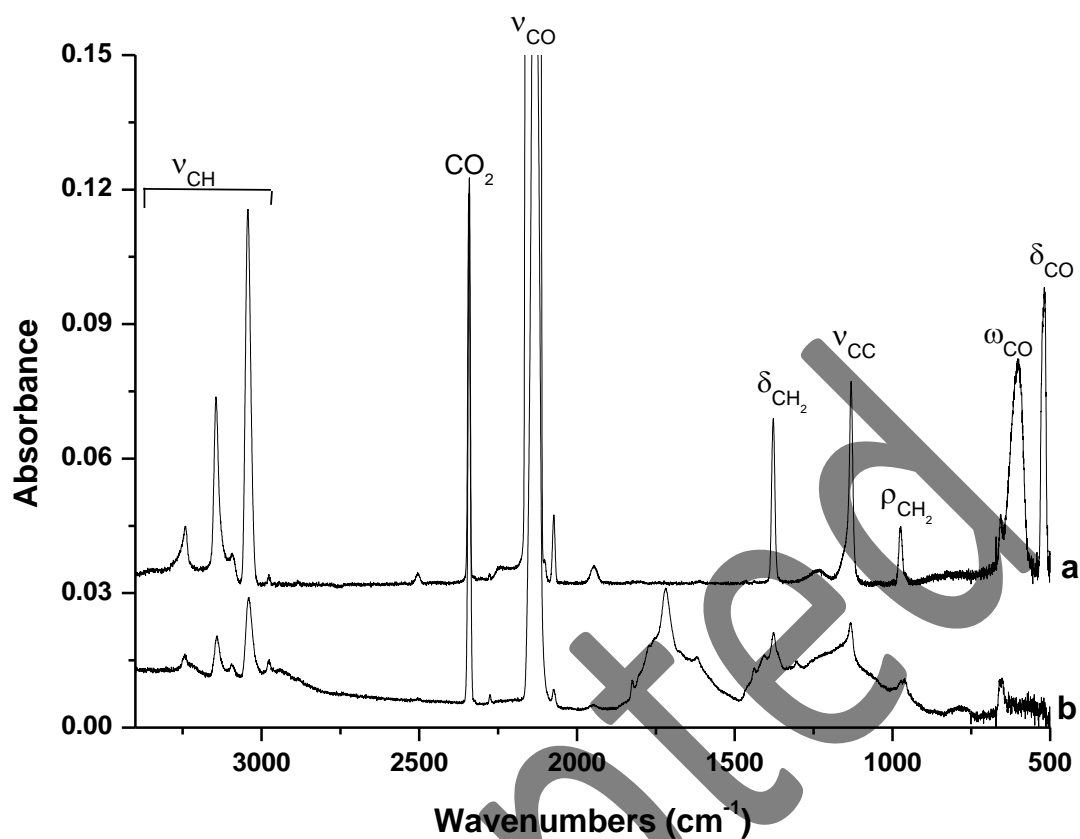


Figure 4: a) IR spectrum of  $\text{CH}_2\text{CO}$  ice formed at 10 K. b) After 30 min photolysis.

However, the results obtained in the first part of the present study can be useful to better characterise the photolysis of ketene ice at 10 K in condensed phase. Figure 5 gathers the IR spectrum of ketene ice irradiated at 10 K and that recorded at 10 K after photolysis of  $\text{CH}_2\text{CO}$  isolated in neon followed by a total sublimation of neon atoms.

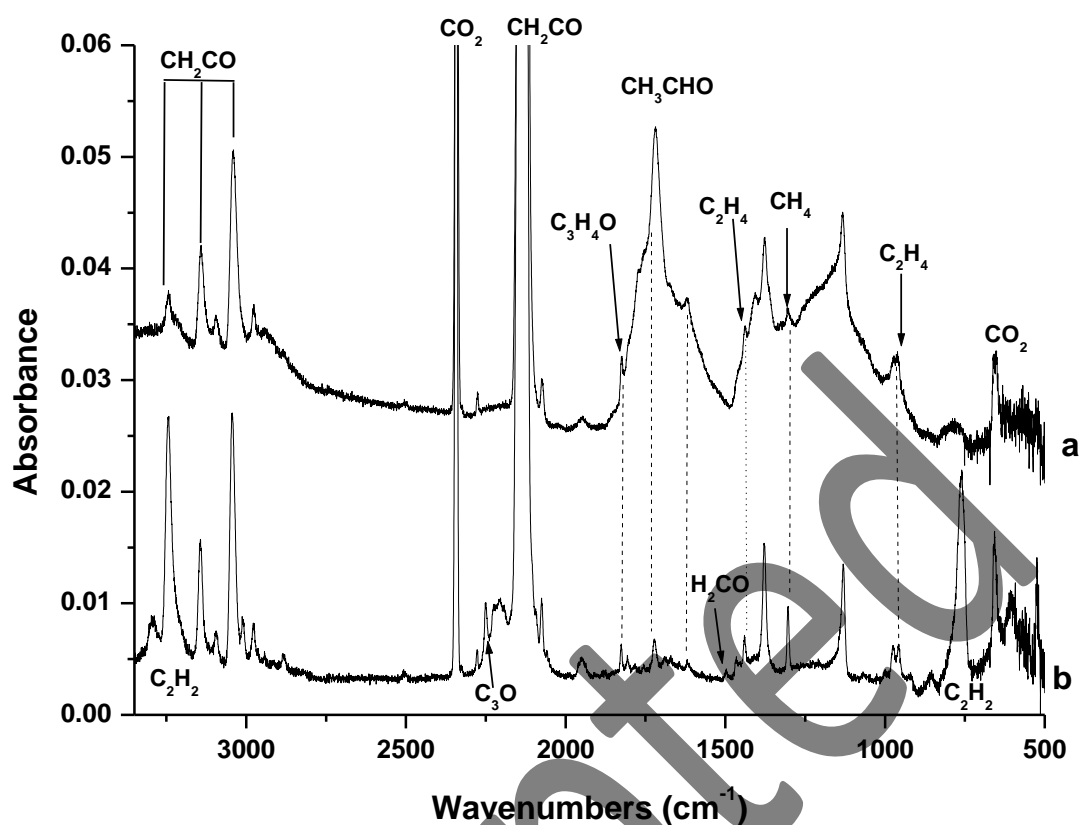


Figure 5: a) IR spectrum recorded at 10 K after photolysis of  $\text{CH}_2\text{CO}$  ice. b) IR spectrum recorded at 10 K after photolysis of  $\text{CH}_2\text{CO}/\text{Ne}$  at 3 K followed by a total sublimation of neon atoms at 20 K, then a cooling down to 10 K.

The comparison between the two spectra (figure 5) recorded at 10 K shows that common chemical species such as  $\text{CH}_3\text{CHO}$ ,  $\text{CH}_4$ ,  $\text{C}_2\text{H}_4$  and  $\text{C}_3\text{H}_4\text{O}$  are formed both in diluted and condensed phase.  $\text{C}_2\text{H}_2$ ,  $\text{C}_3\text{O}$  and  $\text{H}_2\text{CO}$  are not detected during the photolysis of ketene ice and instead a new reaction product with broad absorption bands is observed. Our main goal is to study the nature and evolution of the observed species formed in  $\text{CH}_2\text{CO}_{\text{ice}} + h\nu$  and  $\text{CH}_2\text{CO}/\text{Ne} + h\nu$  reactions. Figure 6 presents the evolution of the infrared spectra obtained during the heating of the  $\text{CH}_2\text{CO}/\text{Ne}$  sample between 10 and 300 K in the 700 - 3400  $\text{cm}^{-1}$  spectral region. It should be noticed that the irradiation of  $\text{CH}_2\text{CO}/\text{Ne}$  has been performed at 3 K and the starting spectrum at 10 K of figure 6 is obtained after the heating of the irradiated sample to 20 K for a total sublimation of the

neon atoms. Afterward the sample is cooled down to 10 K and the spectrum is recorded. As mentioned above, during this heating process from 3 to 20 K, followed by a cooling down to 10 K, new species such as  $C_2H_6$  and  $C_2H_4$  may form with the evaporation of the neon matrix.

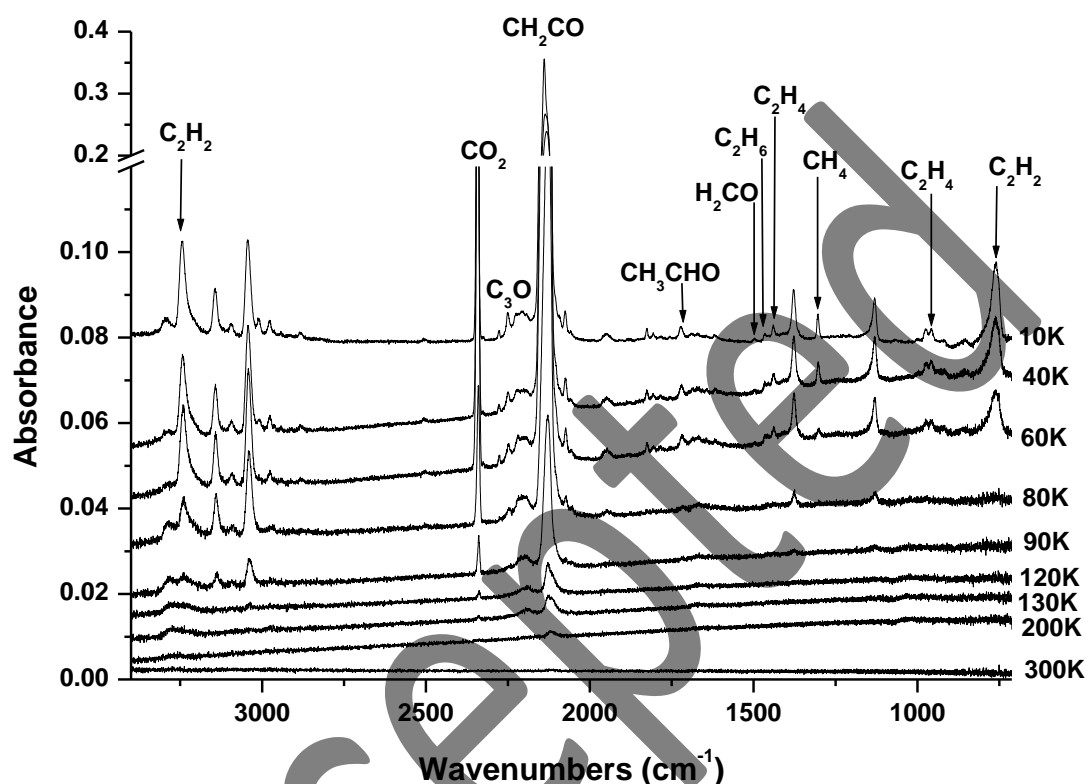


Figure 6: Heating between 10 and 300 K of irradiated  $CH_2CO/Ne$  sample after evaporation of Ne-atoms.

The IR signal of  $CH_4$  starts decreasing at 50 K, and disappears at temperatures higher than 60 K. Then, in the 60-80 K temperature all the photoproducts start desorbing and completely disappear at 80 K.  $CH_2CO$  starts desorbing at 70 K with a maximum of desorption at 95 K and at 120 K only 5% of the total amount of ketene remains trapped in solid phase.

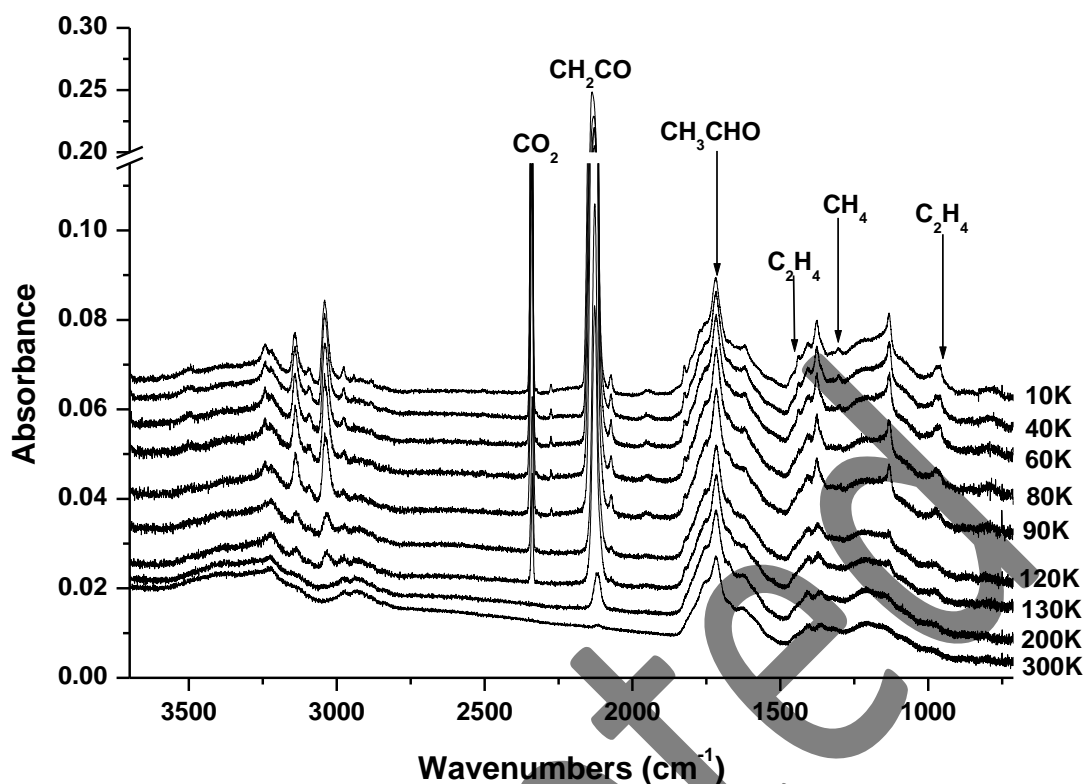


Figure 7: Heating between 10 and 300 K of irradiated  $\text{CH}_2\text{CO}$  ice.

Figure 7 shows the evolution of the infrared spectra obtained during the heating of the irradiated  $\text{CH}_2\text{CO}$  ice between 10 and 300 K. The IR lines associated to  $\text{CH}_4$  and  $\text{C}_2\text{H}_4$  disappear at 80 K while those associated to  $\text{CH}_2\text{CO}$  start decreasing at 90 K. At 120 K, we notice that 1/3 of the total amount of ketene is still trapped in solid phase. This shows that ketene remains stuck in the organic residual products even at temperatures higher than 120 K. In fact, the IR signals associated to ketene disappear progressively during the warming up between 200-300 K. At 300 K the recorded infrared spectrum shows that all the common photoproducts obtained both in diluted and condensed phases have desorbed and only remain the IR signals due to the residual product. The absorption bands of this product can be then characterized properly at 300 K. At this relative high temperature, we notice a wide band, in the C=O stretching region, centred at  $1718\text{ cm}^{-1}$ , with three shoulders at  $1755$ ,  $1672$  and  $1622\text{ cm}^{-1}$ . The other absorption bands are located in the  $\text{CH}_2$  bending region at  $1408$ ,  $1364$ ,  $1317\text{ cm}^{-1}$  and in the C=C and C-O vibrational mode region at  $1202$  and  $1142\text{ cm}^{-1}$ . At 10 K these absorption bands overlap

with the IR signals of CH<sub>2</sub>CO, C<sub>2</sub>H<sub>4</sub> but they remain present in the spectrum recorded 300 K. Furthermore, we have observed two bands in the C-H and OH stretching region between 2800 and 3600 cm<sup>-1</sup>. The spectral positions of these two bands are located 2930 and 3222 cm<sup>-1</sup> and would be assigned to C-H and O-H stretching modes. We summarize in table 4 the spectral positions of the observed absorption bands and their assignments.

Table 4. Spectral positions, vibration modes and intensities of IR features of the organic residues. (vs: very strong, s: strong).

Bands position (cm <sup>-1</sup> )	Vibration modes	Intensity
3377, 3222, 3140	O-H str	s
2979, 2930	C-H str	s
1755	C=O str	s
1718	C=O str	vs
1672	C=O str	s
1622	C=O str	s
1408, 1364, 1317	CH <sub>2</sub> bend	s
1202, 1142	C=C or C-O str	s

Residual organic species are observed only during the photolysis of ketene ice at 10 K. This shows that mechanisms involved in photo-induced reactions of organic molecules depend strongly on the environments where the reactants are trapped.

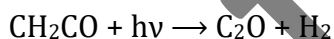
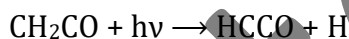
#### 4. Discussion

In this study, we have analyzed the VUV photolysis and thermal processing of CH<sub>2</sub>CO. As already mentioned, the irradiation of CH<sub>2</sub>CO depends strongly on the environment where reactant is trapped. The photolysis of CH<sub>2</sub>CO diluted in neon matrix would imply mechanisms which may be different from those involved during the irradiation of CH<sub>2</sub>CO ice. We have shown that the photolysis of CH<sub>2</sub>CO/Ne at 3 K leads to radical species such as C<sub>4</sub>O, C<sub>3</sub>O, C<sub>2</sub>O, HCCO, HCO, CH<sub>3</sub>CO and stable molecules such as C<sub>2</sub>H<sub>2</sub>, CH<sub>4</sub>, C<sub>2</sub>H<sub>4</sub>, C<sub>2</sub>H<sub>6</sub>, H<sub>2</sub>CO, CH<sub>3</sub>CHO and CO. The IR analysis shows that all the radical species disappear during heating of CH<sub>2</sub>CO/Ne from 3 to 20 K. Then, with the cooling down of the sample

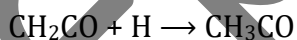
to 10 K, we obtain an ice made of ketene containing C<sub>2</sub>H<sub>2</sub> as the main reaction product, in addition to CH<sub>4</sub>, C<sub>2</sub>H<sub>4</sub>, C<sub>2</sub>H<sub>6</sub>, H<sub>2</sub>CO and CH<sub>3</sub>CHO. One would expect that these same photoproducts would be formed during the photolysis of ketene ice at 10 K. However, we show that the main photoproduct produced during the photolysis of CH<sub>2</sub>CO ice is a residual organic, in addition to CH<sub>4</sub>, C<sub>2</sub>H<sub>4</sub>, C<sub>2</sub>H<sub>6</sub> and CH<sub>3</sub>CHO. In this part, we are going to analyze the mechanisms involved and leading to the formation of the detected photoproducts by focusing on the main ones, namely C<sub>2</sub>H<sub>2</sub> in diluted phase and the residual organics in the condensed phase.

***Mechanisms involved in the diluted phase:***

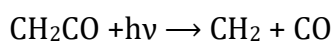
The detection of CCO and HCCO in neon matrix suggests that the photolysis of ketene leads to a dehydrogenation process of CH<sub>2</sub>CO:



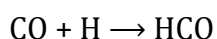
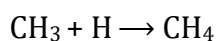
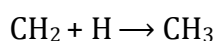
Then the dissociated H-atoms would interact with CH<sub>2</sub>CO to form CH<sub>3</sub>CO and CH<sub>3</sub>CHO, the two species we detect in the neon matrix:

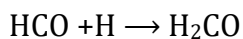


The formation of CH<sub>4</sub> during the photolysis of CH<sub>2</sub>CO/Ne indicate that a second reaction pathway is possible for the photodecomposition of CH<sub>2</sub>CO with a C=C bond cleavage resulting in the formation of CH<sub>2</sub> and CO fragments:



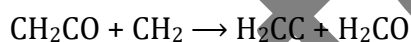
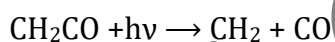
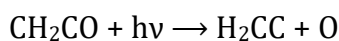
Through hydrogenation processes involving dissociated H-atoms, CH<sub>2</sub> and CO fragments undergo transformation into CH<sub>4</sub>, CHO and H<sub>2</sub>CO, respectively, the three species we detect in neon matrix.





As mentioned earlier,  $\text{CH}_3$  can be a reaction intermediate for  $\text{CH}_4$  through  $\text{CH}_3 + \text{H}$  and also for  $\text{C}_2\text{H}_6$  through  $\text{CH}_3 + \text{CH}_3$ . However, under our experimental conditions, we do not observe the IR absorption corresponding to  $\text{CH}_3$  radical which is located around  $610 \text{ cm}^{-1}$ , a spectral region hidden by  $\text{CH}_2\text{CO}$  absorption bands.

Acetylene  $\text{C}_2\text{H}_2$  is the main reaction product detected after irradiation of  $\text{CH}_2\text{CO}/\text{Ne}$  and its formation is probably due to reactions involving  $\text{H}_2\text{CC}$ , vinylidene radical (Hayes et al. 2001) which may isomerise into  $\text{C}_2\text{H}_2$ . Two reaction pathways may lead to  $\text{H}_2\text{CC}$  (Savchenkova et al. 2019):



### ***Mechanisms involved in the condensed phase:***

The absence of  $\text{C}_2\text{H}_2$  which probably derives from the isomerisation  $\text{H}_2\text{CC}$  radical and the formation of an organic species with  $\text{CO}$ ,  $\text{CH}_2$  and  $\text{OH}$  functional group would suggest that the mechanisms involved in the condensed phase would be related to a self polymerization (Mitchell et al. 2020) of ketene. Mitchell et al. (2020) have shown that different mode of ketene polymerization may take place depending on which functional group is involved in the mechanism: polymerization of  $\text{C}=\text{O}$  generates a polyketene acetal, that of  $\text{C}=\text{C}$  leads to a polyketone while polyester is formed by polymerization of  $\text{C}=\text{O}$  and  $\text{C}=\text{C}$ . All these polymers are stable even at temperatures higher than  $200^\circ\text{C}$  (Conti et al. 1993). However, by analyzing the IR spectrum of the residual product in  $2000\text{-}1600 \text{ cm}^{-1}$  spectral range, we can exclude the formation of diketene under our experimental conditions and support that of a mixture of polyketene acetal, polyketone and polyester. We have synthesised diketene in our laboratory and recorded its IR spectrum (not shown here) which is dominated by two absorption bands at  $1862$  and  $1700 \text{ cm}^{-1}$ . These two IR signals are not observed in our IR spectra (figure 7, spectrum recorded at  $300 \text{ K}$ ) for the ketene ice irradiated. Additionally, the IR spectrum recorded

by Morgen et al. (2020) shows that the  $\nu_{\text{CO}}$  IR signal of polyketone spreads out between 1750 and 1650  $\text{cm}^{-1}$ , with a maximum around 1710  $\text{cm}^{-1}$ . Similarly, Soomro et al. (2014) have shown that polyketone has a wide  $\nu_{\text{CO}}$  absorption band located between 1750 and 1650  $\text{cm}^{-1}$  and centred at 1707  $\text{cm}^{-1}$ . They also showed that spectral position of this absorption band depends strongly on the composition of the polymer chain. It may shift to 1714  $\text{cm}^{-1}$  for polyketone with low CO content and to 1690  $\text{cm}^{-1}$  for polyketone with alternating CO and  $\text{C}_2\text{H}_4$  units. This would suggest that the residual organic we form at 10 K during the photolysis of ketene ice at 10 K would probably be polyketones.

## 5. Astrophysical implications

Several laboratory studies of the photochemistry and thermal processing of interstellar ice analogs have already shown that organic residues with different functional groups (CO, OH, CC, NH,  $\text{NH}_2$ ...) may form at cryogenic temperatures and remain solid at temperatures higher than 300 K. Hagen et al. 1979 have investigated the formation of organic residues containing amino group ( $\text{NH}_2$ ) and carboxyl group (COOH). Allamandola et al. 1988 have observed organic residues with nitrile (CN) and carbonyl (CO) groups. Agarwal et al. 1985 studied organic residuals with alcohol and acid groups using gas chromatography coupled to mass spectrometry (GC-MS), high performance liquid chromatography (HPLC), and near IR spectroscopy. Bernstein et al 1995 have observed an organic material containing 60% HMT ( $\text{C}_6\text{H}_{12}\text{N}_4$ ), 20% ethers and polyoxymethylene (POM) and 20% ketones and amides. Muñoz Caro et al. 2004 have detected new species based on hexamethylenetetramine (HMT,  $\text{C}_6\text{H}_{12}\text{N}_4$ ), they analyzed these new species by GC-MS. Marcellus et al. 2011 have observed small quantities of Hydantoin ( $\text{C}_3\text{H}_4\text{N}_2\text{O}_2$ ) produced from the UV photolysis of ice analogues containing  $\text{H}_2\text{O}$ ,  $\text{CH}_3\text{OH}$  and  $\text{NH}_3$ . Many of these organic compounds have potentially prebiotic implications. Polymer chemistry allows the synthesis of large materials, usually in solutions using initiators and terminators to control the growth of the polymers. We show in this study that self polymerization of ketene take place not in solutions but maybe under interstellar conditions, at cryogenic temperatures. As mentioned in the discussion part, Mitchell et al. (2020) investigated polymerization of ketenes through three mechanisms. The ketene polymerization may take place on  $\text{C}=\text{O}$  to generate a polyketene acetal, on  $\text{C}=\text{C}$  to lead to a polyketone and on both  $\text{C}=\text{O}$  and  $\text{C}=\text{C}$  to form polyester. All these polymers have their melting temperatures in the 200-350°C range.

We show in the present study that the ketene polymerization may also occur through UV photolysis at 10 K. Our results support that ketene interacting with UV photons leads to a mixture of polyketene acetal, polyketone and polyester. These species are stable at high temperatures and they have many functional groups such as (C=C, C=O, C-O-O) which may involve the complex chemistry of the ISM.

## 6. Conclusion

In this study, we have performed the photolysis of ketene under ISM conditions. The irradiated CH<sub>2</sub>CO samples are then heated progressively from 10 to 300 K to investigate the thermally induced reactions. Fourier transform infrared spectroscopy was used to monitor the CH<sub>2</sub>CO + hv reaction. Our main results show that the photolysis of CH<sub>2</sub>CO diluted in a neon matrix at 3 K leads to the formation of radical species such as C<sub>4</sub>O, C<sub>3</sub>O, C<sub>2</sub>O, HCCO, HCO, CH<sub>3</sub>CO and stable molecules such as C<sub>2</sub>H<sub>2</sub>, CH<sub>4</sub>, C<sub>2</sub>H<sub>4</sub>, C<sub>2</sub>H<sub>6</sub>, H<sub>2</sub>CO, CH<sub>3</sub>CHO and CO, respectively, while in the condensed bulk phase, the photoproducts detected are mainly a residual organic, in addition to CH<sub>4</sub>, C<sub>2</sub>H<sub>4</sub>, C<sub>2</sub>H<sub>6</sub>, and CH<sub>3</sub>CHO. We show that the residues formed under our experimental conditions would probably be polyketones. This suggests that photolysis of CH<sub>2</sub>CO at cryogenic temperatures depends strongly on the environments where it is trapped.

## Data availability

The data of this paper will be shared on reasonable request to the corresponding author.

## References

Abusara, Z., Sorensen, T.S., Moazzen-Ahmadi, N., Abusara et al., 2004, Chem. Phys. Lett. 388, 62

Allen, W. D., Schaefer, H. F., III 1986, JCP, 81, 2212

Allen, W. D., Schaefer, H. F., 1988, J. Chem. Phys., 89, 329–344.

Abplanalp M. J. Kaiser, R. I., 2019, Phys. Chem. Chem. Phys., 21, 16949

Allamandola, L. J., Sandford, S. A., Valero, G. J. 1988, Icarus, 76, 225

Agarwal, V. K., Schutte, W., Greenberg, J. M. Ferris, J. P., Briggs, R., Connor, S., Van de Bult, C. P., Baas, F., 1985, *Origins of Life*, 16, 21

Bacmann, A., Taquet, V., Faure, A., Kahane, C., Ceccarelli, C., 2012, *A&A*, 541, L12

Bernstein, M. P., Sandford, S. A., Allamandola, L. J., Chang, S., Scharberg, M. A., 1995, *ApJ*, 454, 327

Botschwina, P., Reisenauer, H. P., 1991 *Chem. Phys Lett* 183, 3

Castillejo, M., Couris, S., Lane, E., Martin, M., Ruiz, J., 1998, *Cheml Phys*, 232, 353

Chen, I.-C., Green, W. H., Jr., Moore, C. B., 1988, *J. Chem. Phys.*, 89, 314

Chen, I.-C., Moore, C. B., 1990, *J. Phys. Chem.*, 94, 263

Chen, I.-C., Moore, C. B., 1990, *J. Phys. Chem.*, 94, 269

Chuang, K., Fedoseev, G., Qasim, D., Ioppolo, S., Jager, C., Henning, Th., Palumbo, M. E., Van Dishoeck, E., Linnartz, H., 2020, *A&A*, 635, A199

Chuang, K., Fedoseev, G., Scirè, C., Baratta, G.A., Jager, C., Henning, Th., Linnartz, H., Palumbo, M. E., 2021, *A&A*, 650, A85

Cole, J. P., Balint-Kurti, G. G., 2003, *J. Chem. Phys.*, 119, 6003

Conti, G., Sommazzi, A., 1993, *J. Mol. Struct.*, 294, 275

Cui, Q., Morokuma, K., 1997, *J. Chem. Phys.*, 107, 4951

Feedoseev, G., Qasim, D., Chuang, K., Ioppolo, S., Lamberts, T., Van Dishoeck, E., Linnartz, H., 2022, *ApJ*, 924:110 (8pp)

Feltham, E. J., Qadiri, R. H., Cottrill, E. E. H., Cook, P. A., Cole, J. P., Balint-Kurti, G. G., Ashfold, M. N. R., 2003, *J. Chem. Phys.*, 119, 6017

Fockenberg, C., 2005, *J. Phys. Chem. A*, 109, 7140

Forsythe, K. M., Gray, S. K., Klippenstein, S. J., Hall, G. E., 2001, *J. Chem. Phys.*, 115, 2134

Glass, G. P., Kumaran, S. S., Michael, J. V., 2000, *J. Phys. Chem. A*, 104, 8360

Golovkin, A.V., Davlyatshin, D.I., Serebrennikova, A.L., Serebrenniko, L.V., 2013, *J. Mol. Struct.*, 1049, 392

Hagen, W., Allamandola, L. J. Greenberg, J. M. 1979, *ApJ*, 65, 215

Haller, I., Pimentel, G. C. 1962, *J. Am. Chem. Soc.*, 84, 2855

Hawkins, M., Andrews, L. 1983, *J. Am. Chem. Soc.*, 105, 2523

Hayes, R. L., Fattal, E., Govind, N., Carter, E. A., 2001, *J. Am. Chem. Soc.*, 123, 641

Herbst, E., van Dishoeck, E., 2009, *Annu. Rev. Astron. Astrophys.*, 47:427

Hudson, R. L., Loeffler, M. J. 2013, *ApJ*, 773, 109

Hudson, R. L., Ferrante, R. F. 2020, *MNRAS*, 492, 283

Irvine, W. M., Friberg, P., Kaifu, N., Kawaguchi, K., Kitamura, Y., Matthews, H. E., Mink, Y., Saito, S., Ukita, N., Yamamoto, S., 1989, *ApJ*, 342, 871

Johansson, L., Andersson, C., Ellder, J., Friberg, P., Hjalmarsen, A., Hoglund, B., Irvine, W. M., Olofsson, H., Rydbeck, G., 1984, *A&A*, 130, 227

Jonusas, M., Krim, L., *MNRAS*, 2017, 470, 4564

Kaledin, A. L., Seong, J., Morokuma, K., 2001, *J. Phys. Chem. A*, 105, 2731

Khoshkhoo H., Nixon E.R., 1973. *Spectrochim. Acta Part A*, 29, 4, 603

Kim, S. K., Choi, Y. S., Pibel, C. D., Zheng, Q. K., Moore, C. B. J., 1991, *Chem. Phys.*, 94, 1954

Kim, S. K., Lovejoy, E. R., Moore, C. B., 1995, *J. Chem. Phys.*, 102, 3202

Klippenstein, S. J., East, A. L. L.; Allen, W. D., 1996, *J. Chem. Phys.*, 105, 118

Klippenstein, S. J., Marcus, R. A., 1989, *J. Chem. Phys.*, 91, 2280

Lin, M.Y., Lo, J.I., Lu, H.C., Chou, S.L., Peng, Y.C., Cheng, B.M., Ogilvie, J. F., 2014, *J. Phys. Chem. A*, 118, 3438

Liu, X., Westre, S. G., Getty, J. D., Kelly, P. B., 1992, *Chem. Phys. Lett.*, 188, 42

Liu, J., Wang, F. Y., Wang, H., Jiang, B., Yang, X. M., 2005, *J. Chem. Phys.*, 122, 104309

Liu, Y., Yu, J. K., Huang, X. R., Sun, C. C., 2006, *J. Chem. Phys.*, 125, 044311

Lovejoy, E. R., Kim, S. K., Moore, C. B., 1992, *Science*, 256, 1541

Maier, G., Reisenauer, H.P., Schafer, U., Balli, H., 1988, *Angew. Chem.*, 100, 4, 590

Maity, S., Kaiser, R. I., Jones, B. M., 2014, *ApJ*, 789, 36

Marcellus, P., Bertrand, M., Nuevo, M., Westall, F., Hendecourt, L. L. S., 2011, *Astrobiology*, 11, 847

Marshall, M. D., McKellar, A. R. W., 1986, *J. Chem. Phys.*, 85, 7, 3716

Matthews, H., Sears, T., 1986, *ApJ*, 300, 766

Mitchell, S. M., Niradha Sachinthan, K. A., Pulukkody, R., Pentzer, E. B., 2020, *ACS Macro Lett.*, 9, 1046

Moore, C. B., Pimentel, G. C., 1963, JCP, 38, 2816

Moreno, I. G., Lovejoy, E. R., Moore, C. B., 1994, J. Chem. Phys., 100, 8902

Morgan, C.G., Drabbels, M., Wodtke, A. M., 1996, J. Chem. Phys., 105, 4550

Morgen, T. O., Baur, M., Göttker-Schnetmann, I., Mecking, S., 2020, Nature 11, 3693

Muller, S., Beelen, A., Guélin, M., Aalto, S., Black, J. H., Combes, F., Curran, S. J., Theule, P., Longmore, S. N., 2011, A&A, 535, A103

Muñoz Caro, G. M., Meierhenrich, U. J., Schutte, W. A., Thiemann, W. H.-P., Greenberg, J. M., 2004, A&A, 413, 209

Ogihara, Y., Yamamoto, T., Kato, S., 2011, Chem. Phys. Lett., 511, 28

Ogihara, Y., Yamamoto, T., Kato, S., 2011, J. Chem. Theory Comput., 7, 2507

Ohishi, M., Kawaguchi, K., Kaifu, N., et al. 1991, in ASP Conf. Ser. 16, Atoms, Ions and Molecules: New Results in Spectral Line Astrophysics (San Francisco, CA: ASP), 387

Pereira R. C., de Barros A. L. F., da Costa C. A. P., Oliveira P. R. B., Fulvio D., da Silveira E. F. 2020 MNRAS 495, 40

Petek, H., Nesbitt, D. J., Darwin, D. C., Ogilby, P. R., Moore, C. B., 1989, J. Chem. Phys., 91, 11, 6566

Pirim C., Krim L., 2011, PCCP, 13, 19454

Rouillé, G., Jäger, C., and Henning, Th., 2020, The ApJ, 892:96

Savchenkova, A. S., Semenikhin, A. S., Chechet, I. V., Matveev, S. G., Konnov, A. A., Mebel, A. M., 2019, J. Comput. Chem., 40, 387

Schrivver, A., Coanga, J. M., Schrivver, L., Ehrenfreund, P., 2004, Chem. Phys., 303, 13

Singmaster, K. A., and Pimentel, G. C., 1989, J. Mol. Struct., 194, 215

Soomro, S. S., Cozzula, D., Leitner, W., Vogta, H. Müller, T. E., 2014, Polym. Chem., 5, 3831

Turner, B., 1977, ApJL, 213, L75.

Turner, B., Terzieva, R., Herbst, E., 1999, ApJ, 518, 699

Turner, A. M., Koutsogiannis, A. S., Kleimeier, N. F., Bergantini, A., Zhu, C., Fortenberry, R. C., Kaiser, R. I., 2020, ApJ, 896, 88

Wu, Y. J., Chen, H. F., Camacho, C., Witek, H. A., Hsu, S. C., Lin, M. Y., Chou, S. L., Ogilvie, J. F., Cheng, B. M., 2009, Astro-phys., J. 701, 8

Xiao, H., S. Maeda, S., Morokuma, K., 2013, J. Phys. Chem. A, 117, 32, 7001

Yamabe, S., Morokuma, K., 1978, J. Am. Chem. Soc., 100, 24, 7551

Yarkony, D. R., 1999, J. Phys. Chem. A, 103, 6658

Yu, J., Klimppenstein, S. J., J., 1991, Phys. Chem., 95, 9882

Zasimov, P. V., Ryazantsev, S. V., Tyurin, D. A., Feldman, V. I., 2020, MNRAS, 491, 514

Zasimov, P. V., Sanochkina, E. V., Feldman, V. I., 2022, PCCP., 24, 419

accepted